Microstructural and Mechanical Characterization of Magnesium-AZ31 Alloy Reinforced with Carbon Nanotubes and Nano-Hydroxyapatite

Ashu Tyagi
Department of Mechanical Engineering, Deenbandhu Chhotu Ram University of Science & Technology

Pardeep Kumar
Department of Mechanical Engineering, Deenbandhu Chhotu Ram University of Science & Technology

https://doi.org/10.5109/7388838

出版情報：Evergreen. 12 (3), pp.1418-1425, 2025-09. 九州大学グリーンテクノロジー研究教育センター
バージョン：

Microstructural and Mechanical Characterization of Magnesium-AZ31 Alloy Reinforced with Carbon Nanotubes and Nano-Hydroxyapatite

Ashu Tyagi[1], Pardeep Kumar[1,*]

[1]Department of Mechanical Engineering, Deenbandhu Chhotu Ram University of Science & Technology, Murthal, Sonipat, Haryana, India-131039, India

*Author to whom correspondence should be addressed:
E-mail: pardeepkumar.me@dcrustm.org

(Received September 26, 2024; Revised August 06, 2025; Accepted September 13, 2025)

Abstract: Strength-to-weight ratio has always been a key concern in the automotive and aerospace sector. Therefore in metal matrix composite (MMC), magnesium, aluminum, titanium always being preferred as matrix material. Although aluminum as a matrix material remain the first choice and is widely used by researchers because of the ease of fabrication in comparison to magnesium and titanium metal matrix composite. But magnesium is also an attractive material in terms of its properties as it is 36% and 78% lighter per unit volume than aluminum and iron respectively. Therefore the present study has investigated the effect of reinforcements such as Carbon Nanotubes (CNT) and Nano-Hydroxyapatite (nHA) on the mechanical properties of magnesium alloys based composites. Various properties have been studied, and found significant improvements were found in the developed composite. Furthermore, the microstructures of hybrid composite materials were examined using scanning electron microscopy (SEM). The chemical analysis and distribution of reinforcement were performed using EDX.

Keywords: Composite; Magnesium alloy; Mechanical properties; Nanostructures Reinforcements; Stir casting

1. Introduction

Material selection for various components in applications such as automobiles, power plants, sheet metals, and defense sectors is an intricate and difficult task, owing to a variety of factors such as fuel economy, safety enhancements, overall cost considerations etc[1)]. Magnesium Metal Matrix Composites (MMCs) have emerged as crucial materials in various sectors due to their distinct and favorable features, such as a high strength-to-weight ratio, good wear resistance, and low cost, which have resulted in a significant increase in demand for magnesium-based composites[2,3)]. The use of lightweight materials has not only reduced weight but has also resulted in a slew of advancements, including improved vehicle drivability, fuel efficiency and the major concern of CO_2 emissions. The automobile industry is actively transitioning a way from largely steel-based products and towards lightweight materials such as magnesium and its composites[4)]. Magnesium is preferred for its light weight qualities, has great potential as a feasible material for the development of lightweight structural components, which are in high demand in both the aerospace and automotive sectors[5,6)]. Magnesium has a significant benefit over aluminium as a result, substituting aluminium components with magnesium materials can result in significant savings in fuel consumption, making such a move financially viable[7,8)]. It is worth mentioning that the usage of magnesium-based materials was hampered by their low ductility, which resulted in a restriction by the Federal Aviation Administration (FAA) in 2015[9,10)]. Nonetheless, magnesium alloys have a wide range of uses, notably in the aircraft industry[11,12)].

Numerous techniques have been investigated and address the manufacturing of magnesium-based composites[13,14)]. Among them, the liquid-phase stir-casting process has acquired general popularity as an efficient method for producing magnesium-based composites[15,16)]. This technology enables the inclusion of reinforcing elements as well as the attainment of desired mechanical characteristics, making it a vital tool for the improvement of magnesium composite materials in a variety of industrial applications[17,18)].

In 1930 first time L. Chevrolet used the magnesium-based piston for racing cars. Beetle car have also used the magenisium-based casting for making the transmission

Cite: A. Tyagi, P. Kumar, "Microstructural and Mechanical Characterization of Magnesium-AZ31 Alloy Reinforced with Carbon Nanotubes and Nano-Hydroxyapatite". Evergreen, 12 (03) 1418-1425 (2025). https://doi.org/10.5109/7388838.

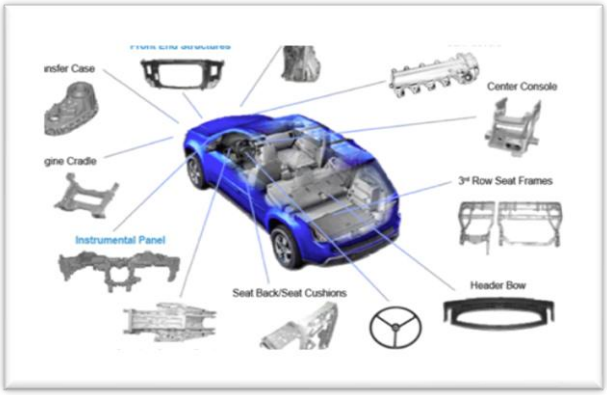

Fig.1: Application of Mg-Based Components in automobile

and crankcase [A]. Further Audi A4, A6 and Ford's truck gear box housing, cylinder head of the V8 engine etc. have used the Mg based casting for various components in automobile [B]. By the 1990s, many more parts and products have been possible to cast such as seat, frames, CCB's, steering wheels and many more as shown in Figure 1.

Therefore keeping in view of wide application of Mg Alloys in the automobile industry, an attempt has been made to synthesize the Mg based composite for the automotive applications[19]. There are various methods of fabrication of metal matrix including stir casting, infiltration, and squeeze casting. The conventional stir casting process is a popular approach for composite manufacture because of its versatility in making complicated designs as well as its low cost[20,21]. Metal matrix composites have found widespread use in a variety of industries, including automotive, aircraft, sporting goods, and manufacturing[22,23]. Nonetheless, ongoing attempts are undertaken to improve current MMCs and produce unique versions tailored to a wide range of applications[24-27].

2. Materials and Methods

This present research work explores the influences of reinforced material such as CNT and nHA with the matrix material AZ31 magnesium alloy. The bottom pouring stir casting process has been used for the synthesis of composite material.

2.1. Determination of Reinforcement Compositions

In this article, we used two different reinforcements to construct a total of seven composite samples. Previous research in the subject has used varying amounts of these reinforcements in powdered form.

Table 1 offers a detailed overview of the composition of these reinforcements, describing the two types of reinforcements used in the manufacture of the composite specimens, as well as their corresponding amounts. The different quantities of these reinforcements are crucial in defining the resultant characteristics of the composite materials[28-31], and Table 1 is a useful reference for understanding the exact formulations used in our investigation. This methodical approach to reinforcement composition enables us to systematically investigate the effect of different reinforcement ratios on the mechanical and structural properties of the composite specimens, contributing to a better understanding of the materials and their potential applications in various engineering contexts[32-34].

Table 2 summarizes the components of the seven unique composite specimens under consideration in this study. With values in grams, these compositions have been precisely computed for the manufacture of composites utilizing the stir casting process. Table 2 meticulously documents the total weight of each composite sample, providing insight into precise quantity of each constituent material, including the matrix material and the reinforcements, in the composite specimens. This precise breakdown of the composite composition is critical for understanding the unique formulations used in our study, which affect the mechanical and structural properties of the

Table 1: Reinforcement Compositions

S.N.	Material	Reinforcements	Wt. %
1.	AZ31	CNT & nHA	(0% CNT + 0% nHA) = 0%
2.	AZ31	CNT & nHA	(3% CNT + 0% nHA) = 3%
3.	AZ31	CNT & nHA	(4.5% CNT + 0% nHA) = 4.5%
4.	AZ31	CNT & nHA	(6% CNT + 0.5% nHA) = 6.5%
5.	AZ31	CNT & nHA	(7.5% CNT + 0.25% nHA) = 7.75%
6.	AZ31	CNT & nHA	(7.5% CNT + 0.5% nHA) = 8%
7.	AZ31	CNT & nHA	(12% CNT + 0.5% nHA) = 12.5%

Cite: A. Tyagi, P. Kumar, "Microstructural and Mechanical Characterization of Magnesium-AZ31 Alloy Reinforced with Carbon Nanotubes and Nano-Hydroxyapatite". Evergreen, 12 (03) 1418-1425 (2025). https://doi.org/10.5109/7388838.

Table 2: Composite Specimen Compositions

S.N.	AZ31	CNT	nHA	Total wt. (g)
1	500gm	0	0	500
2	500gm	15gm	0	515
3	500gm	22.5gm	0	522.5
4	500gm	30gm	2.5gm	532.5
5	500gm	37.5gm	1.25gm	538.75
6	500gm	37.5gm	2.5gm	540
7	500gm	60gm	2.5gm	562.5

final composite materials. By publishing this quantitative information in Table 2, we want to promote a thorough understanding of our experimental design and technique, providing significant insights for mechanical engineering and materials science researchers and practitioners.

2.2. Fabrication of AZ31/CNT/nHA

In the process of creating composite materials, the reinforcements, normally in powdered form, are injected into the magnesium metal matrix and fully mixed by agitation, which is frequently performed using a mechanical stirrer. Following the conclusion of this blending process, the molten liquid is cast into a mould of the appropriate shape, using different casting processes such as permanent mould casting, die casting, or sand casting to produce the necessary geometry[35-37]. The photographic view of stir casting apparatus is shown in Figure 2.

To better understand the stir casting process for the manufacturing of composite materials, we started with an AZ31 magnesium sheet. We waited anxiously for the stir casting furnace to reach 500°C. Following that, the magnesium sheet was placed in the crucible and heated until it reached 900°C. At this point, the reinforcing powders were added to the molten magnesium and rapidly agitated for 10 minutes to ensure thorough and homogeneous mixing of these enforcements with the base material. Following this mixing process, it took around 4 to 5 hours to create a single composite specimen for casting into a cylindrical mould. After that, the casting was allowed to cool and harden for around 3 hours. This procedure was followed for all five composite samples.

The key to this method is melting the base metal within the stir casting furnace and introducing the reinforcements at a regulated temperature of 500°C. This mixing of molten metal and reinforcements, followed by casting into a cylindrical mould, ensures the production of composite specimens with the necessary properties and geometry. Due to the extremely high melting temperature of the metal, which in this case approaches 900°C, extreme caution and safety measures must be properly followed during the casting process. This emphasis on safety emphasizes the significance of a regulated and methodically conducted procedure when working with materials at such extreme temperatures, therefore limiting possible dangers and assuring the effective manufacturing of composite materials.

Fig. 2: Stir Casting Apparatus

Table 3: Casting Process Parameter

Parameter	Approx. Value
Maximum temperature of stirring	900°C
Reinforcement preheat temperature	500°C
Stirrer speed	250 rpm
Time for stirring	10 minutes
Mould preheat temperature	260°C
First casting preparation time	4 hours
Second casting preparation time	4 hours
Third casting preparation time	4 hours
Fourth casting preparation time	4 hours
Pouring time for the liquid composite into the mould	10 seconds
Cooling time of casted composite	2.5-3hours

Table 3 showing the specific values of the stir casting parameters used throughout this research endeavour. These factors shape the features and qualities of the resultant composite materials; therefore their precise selection and control are critical to the production process. Several essential concerns and processes deserve special attention during the manufacturing process. These include careful control of the stirring time, temperature regimes, and the order in which the reinforcing ingredients are added and mixed[38-40].

3. Results and Discussions

This study involved a thorough analysis of the mechanical characteristics of the materials that were being investigated. Thorough testing was conducted on critical mechanical properties such hardness, density, and porosity in order to obtain a thorough understanding of the materials' performance characteristics.

To determine the materials' ability to endure applied stresses and resist deformation, hardness testing was done.

Cite: A. Tyagi, P. Kumar, "Microstructural and Mechanical Characterization of Magnesium-AZ31 Alloy Reinforced with Carbon Nanotubes and Nano-Hydroxyapatite". Evergreen, 12 (03) 1418-1425 (2025). https://doi.org/10.5109/7388838.

The information obtained from these hardness tests is essential for assessing the strength and resilience of the materials, two essential characteristics determining their appropriateness for a wide variety of technical uses. Together with hardness evaluations, density readings were carefully obtained, yielding a precise mass/volume ratio for the materials. When it comes to determining a material's weight-related properties and structural integrity, density is a crucial factor. For this reason, it is relevant in situations where weight is of utmost importance.

Moreover, in addition to these basic evaluations of mechanical properties, we also carried out morphological and chemical tests to further explore the materials' microstructural and compositional details. On the other hand, chemical analysis provided important insights into the materials' overall performance, durability, and possible reactivity in various environmental situations by illuminating the elements' composition and bonding properties.

3.1. Hardness Test

To assess the hardness of the composite materials under study in our research, we used a hardness tester. Specifically, we tested the hardness of four different samples with different weight percentages of reinforcements that is, 3%, 4.5%, 6.5%, 7.75%, 8%, and 12.5%. The test findings demonstrated a noteworthy pattern in which the hardness values increased in tandem with the rise in the proportion of reinforcements in the composite.

A Microvicker Hardness tester with a 1/16-inch ball diameter and a 100 kgf (kilogram-force) load was used to perform the hardness tests which can be shown in Figure 4. The tests were conducted at various locations on the surface of each sample in order to guarantee the representativeness and robustness of the hardness evaluations.

Fig. 3: Vickers indentation Mark

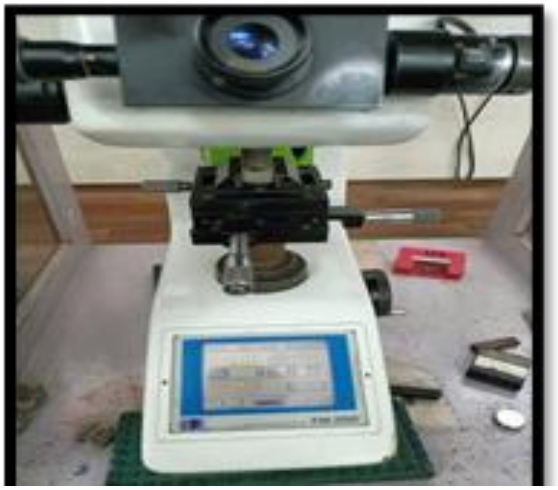

Fig. 4: Microvicker Hardness Tester

For ten seconds during the test, the applied force was continuously maintained. After the indentation procedure, optical examination was performed on the resulting indentations[41]. We were able to precisely measure the size and extent of the depression by measuring the imprints' diagonal lengths throughout this study. The hardness values acquired by means of this methodical testing process provide useful information about the materials' resistance to external forces and capacity to tolerate localised deformation, illuminating their mechanical characteristics and appropriateness for certain technical uses. An essential component of our study findings is the pattern we saw of increased hardness with larger percentages of reinforcement. This provides valuable insights into the improved mechanical performance of these composites[42]. The Vickers indentation mark has been seen well defined in the Mg-AZ31 alloy-based hybrid composite reinforced with a mixture of carbon nanotubes (CNTs) and nano-hydroxyapatite (nHA) particles, showed in Figure 3. The indentation shows a proof of material being resistant to localized plastic deformation. The hardness properties, determined with the help of the Vickers test method (54 HV on average), provided information about a significant surface hardening of the composite relative to unmodified Mg-AZ31 alloy. The improvement mainly arises from the homogeneous distribution of CNTs as load-bearing reinforcements and nHA nanoparticles, which are effective in grain-refinement and dislocation blocking. Similarly, the presence of indenter marks indicates that the matrix had bonded well to reinforcements which too is in agreement with the enhanced hardness and composite mechanical integrity.

3.2. Density and porosity measurement

The theoretical density of magnesium composites was calculated using the rule of mixtures. The actual density of pure AZ31 and composite were calculated using Archimedes' principle. The cylindrical sample was

Cite: A. Tyagi, P. Kumar, "Microstructural and Mechanical Characterization of Magnesium-AZ31 Alloy Reinforced with Carbon Nanotubes and Nano-Hydroxyapatite". Evergreen, 12 (03) 1418-1425 (2025). https://doi.org/10.5109/7388838.

weighed in air (W_a), then suspended in distilled water and weighed again (W_w). The actual density was calculated according to equation 1.

$$\rho_a = (W_a/(W_a - W_w)) \times \rho_w \quad (1)$$

Where ρ_a is the actual density and ρ_w is the density of water.

The sample was weighed using a photoelectric balance with an accuracy of 0.1 mg.

In accordance with Eq. (1), the actual density of each material can be calculated; theoretical density (ρ_t) of material was calculated by the ratio of mass to volume.

The porosity of each material can be calculated according to equation 2.

$$P = 1 - (\rho_a/\rho_t) \quad (2)$$

Where P is the porosity of the material, ρ_a is the actual density and ρ_t is the theoretical density.

Table 4: Results of hardness, density and porosity

Grade	% of Reinforcement	Result (HV)	Density (g/cc)	Porosity
AZ31	0	40	1.8091	1.42
AZ31	3	42	1.8101	1.38
AZ31	4.5	44.5	1.8197	1.34
AZ31	6.5	47	1.8231	1.26
AZ31	7.75	49	1.8249	1.11
AZ31	8	52	1.8310	.98
AZ31	12.5	54	1.8397	.86

Table 4 shows that increasing reinforcement in AZ31 alloy enhances hardness from 40 to 54 HV and slightly increases density. Porosity decreases significantly from 1.42% to 0.86%, indicating improved densification and reduced voids due to effective dispersion of reinforcements. It is clear from the data on AZ31 composite materials that adding reinforcement, even at a percentage of 12.5%, causes the hardness (HV) to climb steadily and significantly, to 54 HV for the composite with 12.5% reinforcement. This positive connection demonstrates how reinforcing effectively affects the hardness of the material. Moreover, higher reinforcement percentages are associated with a little rise in density and a decrease in porosity, both of which indicate enhanced material compactness. The composite that has 12.5% reinforcement stands out as being ideal since it has the maximum hardness of 54 HV, the lowest density of 1.8397 g/cc, and the least amount of porosity at 0.86%. Together, these results highlight how well reinforcing works to improve the mechanical characteristics of AZ31 composites. Significant information may be gained from the trends in hardness, density, and porosity to optimise composite formulations to satisfy particular performance requirements, especially in applications where controlled material density and enhanced hardness are critical factors In summary, the findings highlight how well reinforcing may improve the mechanical characteristics of AZ31 composites. The hardness, density, and porosity patterns that have been identified offer important information for fine-tuning composite formulations to satisfy certain performance standards. These formulations may find use in applications where precise material density and enhanced hardness are essential. This passage is a solitary paragraph

3.3. SEM analysis

SEM, or scanning electron microscopy, is an essential instrument for exploring the complex morphological properties of materials. This method provides a thorough picture of a sample's microstructure by carefully scanning the sample's surface with electrons. Particle distributions of metallic and non-metallic components can be clarified by use of SEM imaging. Magnified at 500x, 1000x, 2500x, and 5000x, the Scanning Electron Microscopy micrograph in Figure 5.

Figure 5 exhibit the even dispersion of carbon nanotubes (CNTs) and nano-hydroxyapatite (nHA) particles in the matrix of Mg-AZ31 alloy. Elongated structures denote CNTs which provide load transfer and mechanical strenghtening, while dispersed clusters signify nHA particles for grain refinement and dislocation pinning.

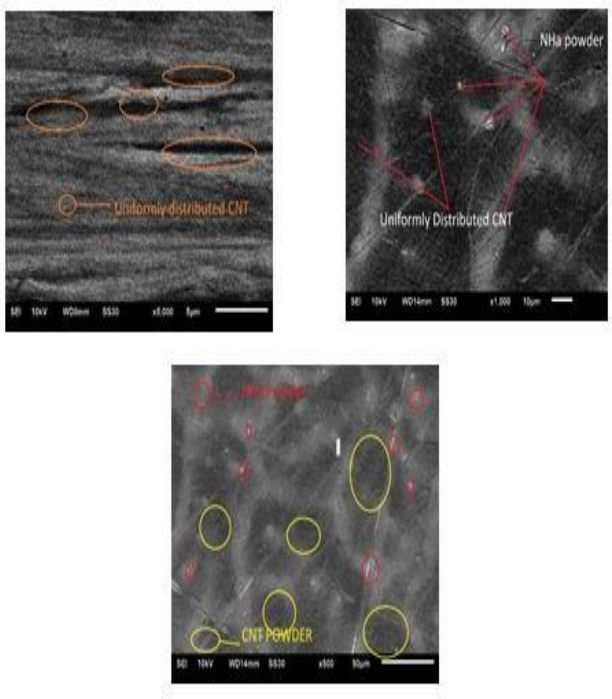

Fig. 5: SEM micrograph of Developed AZ31 composite

Cite: A. Tyagi, P. Kumar, "Microstructural and Mechanical Characterization of Magnesium-AZ31 Alloy Reinforced with Carbon Nanotubes and Nano-Hydroxyapatite". Evergreen, 12 (03) 1418-1425 (2025). https://doi.org/10.5109/7388838.

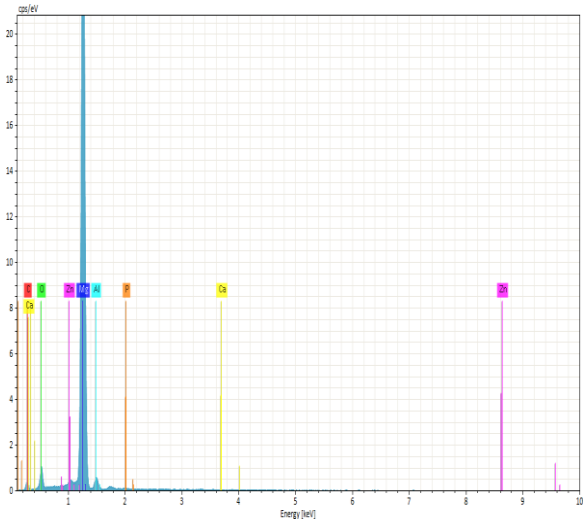

Fig. 6: EDX map of developed composite

The uniform distribution of both reinforcements suggests that they were well-mixed, and the good interfacial bonding between reinforcements and matrix contribute to microstructure stability and the final properties. Understanding the material's composition, structural integrity, and its uses in a range of scientific and technical fields is made possible by these tiny insights.

3.4. EDX analysis

The Energy Dispersive X-ray Spectroscopy (EDX) data are shown in Figure 6, providing a thorough understanding of the elemental makeup of the AZ31/CNT/nHA composites. There are four samples in the EDS analysis, and each has a unique weight %. Interestingly, the pictures show very low-intensity oxygen peaks, indicating that the composites were effectively shielded from ambient oxygen trapping during the production process. This shield is created by the methodical stirring process that is carried out through a tiny opening on top of the furnace, in addition to the melting process occurring inside of a sealed chamber. As shown in the following Figure, argon gas shielding was used to further reduce the danger of magnesium oxidation. The EDS spectra clearly demonstrate that the composite specimens contain particles of calcium (Ca), phosphorus (P), and carbon (C). Surprisingly, as reinforcement increases, an upward trend in the content peaks of C, P, and Ca is shown, suggesting that the reinforcement particles are better dispersed throughout the magnesium matrix. These results highlight how well the manufacturing process preserves the composite material's integrity and guarantees a consistent dispersion of reinforcing components.

4. Conclusions and Future scope

The present study's findings highlight a number of important implications. To get the best outcomes in the composite material, it is crucial to first maintain the correct ratios between the matrix and reinforcement weight percentages. The results of the investigation show that hardness exhibit a significant rise with increasing reinforcement content, peaking at 12.5% by weight of reinforcements. Furthermore, when the percentage of reinforcement increases, the elongation percentage decreases and reaches a minimum at the 12.5% weight of reinforcement. The study emphasises how efficient and cost-effective the stir casting process is for creating Metal Matrix Composites (MMCs). This approach seems to be both simple to use and financially feasible for producing Magnesium Matrix Composites (MMCs). Additionally, when reinforced with 12.5% by weight, the microstructural study performed using Energy Dispersive X-ray Spectroscopy (EDX) and Scanning Electron Microscopy (SEM) showed a homogeneous distribution of particles in the composite material. Together, these discoveries advance our knowledge of the mechanical and microstructural properties of magnesium-based composites reinforced with nano-hydroxyapatite and carbon nanotubes.

Reinforcement ratios may also be optimized in future studies, as well investigating dynamic mechanical behavior and corrosion resistance under service conditions. Such an evidence can be enriched by means of advanced characterization techniques and numerical modeling to gain a fair understanding on the underlying microstructural mechanisms. Moreover, studies investigating real-world applications in areas like automotive, aerospace and biomedical will push the laboratory-based discoveries closer to industry-scale deployment.

Acknowledgements

The authors acknowledge that no financial support to any agency or concerned institute for the research, authorship, and publishing of this manuscript.

Conflict of interest

The authors have no conflict of interest in the research, authorship, writing and publishing of this manuscript.

References

1) M.K. Gupta, V. Singhal, and N.S. Rajput, “Applications and challenges of carbon-fibres reinforced composites: a review,” Evergreen, 9 (3) 682–693 (2022). doi:10.5109/4843099.
2) D.S. Patil, and M.M. Bhoomkar, “Investigation on mechanical behaviour of fiber-reinforced advanced polymer composite materials,” Evergreen, 10 (1) 55–62 (2023). doi:10.5109/6781040.
3) M.C. Şenel, M. Gürbüz, and E. Koç, “Fabrication and characterization of synergistic al-sic-gnps hybrid composites,” Compos. Part B Eng., 154 1–9 (2018). doi:10.1016/j.compositesb.2018.07.035.

4) V.B. Mohan, K. tak Lau, D. Hui, and D. Bhattacharyya, “Graphene-based materials and their composites: a review on production, applications and product limitations,” Compos. Part B Eng., 142 200–220 (2018). doi:10.1016/j.compositesb.2018.01.013.
5) K.S. Novoselov, A.K. Geim, S. V. Morozov, D. Jiang, M.I. Katsnelson, I. V. Grigorieva, S. V. Dubonos, and A.A. Firsov, “Two-dimensional gas of massless dirac fermions in graphene,” Nature, 438 (7065) 197–200 (2005). doi:10.1038/nature04233.
6) K.S. Novoselov et al, “Electric field effect in atomically thin carbon films,” 306 (5696) 666–669 (2016).
7) Gosh Alexander A, Bao Suchismita, Calizo Wenzhong, Teweldebrhan Irene, Miao Desalegne, Lau Feng, and Nig Chun, “Superior thermal conductivity of single-layer graphene,” Nano Lett., 8 (3) 902–907 (2008).
8) H. Sosiati, N.D.M. Yuniar, D. Saputra, and S. Hamdan, “The influence of carbon fiber content on the tensile, flexural, and thermal properties of the sisal/pmma composites,” Evergreen, 9 (1) 32–40 (2022). doi:10.5109/4774214.
9) A. Mahyudin, S. Arief, H. Abral, Emriadi, M. Muldarisnur, and M.P. Artika, “Mechanical properties and biodegradability of areca nut fiber-reinforced polymer blend composites,” Evergreen, 7 (3) 366–372 (2020). doi:10.5109/4068618.
10) H. Sosiati, Y.A. Shofie, and A.W. Nugroho, “Tensile properties of kenaf/e-glass reinforced hybrid polypropylene (pp) composites with different fiber loading,” Evergreen, 5 (2) 1–5 (2018). doi:10.5109/1936210.
11) C. Lee, X. Wei, J.W. Kysar, and J. Hone, “Measurement of the elastic properties and intrinsic strength of monolayer graphene,” Science (80-.)., 321 (5887) 385–388 (2008). doi:10.1126/science.1157996.
12) A. Saboori, M. Pavese, C. Badini, and P. Fino, “A novel approach to enhance the mechanical strength and electrical and thermal conductivity of cu-gnp nanocomposites,” Metall. Mater. Trans. A Phys. Metall. Mater. Sci., 49 (1) 333–345 (2018). doi:10.1007/s11661-017-4409-y.
13) M.C. ŞENEL, and M. GÜRBÜZ, “Investigation on mechanical properties and microstructures of aluminum hybrid composites reinforced with al2o3/gnps binary particles,” Arch. Metall. Mater., 66 (1) 97–106 (2021). doi:10.24425/amm.2021.134764.
14) Y. Zhu, S. Murali, W. Cai, X. Li, J.W. Suk, J.R. Potts, and R.S. Ruoff, “Graphene and graphene oxide: synthesis, properties, and applications,” Adv. Mater., 22 (35) 3906–3924 (2010). doi:10.1002/adma.201001068.
15) S. Nayak, and M.P. Kumar, “Mechanical characterization and static analysis of natural fiber based composite propeller blade,” Evergreen, 10 (2) 805–812 (2023). doi:10.5109/6792832.
16) M. Wang, Y. Zhao, L.D. Wang, Y.P. Zhu, X.J. Wang, J. Sheng, Z.Y. Yang, H.L. Shi, Z.D. Shi, and W.D. Fei, “Achieving high strength and ductility in graphene/magnesium composite via an in-situ reaction wetting process,” Carbon N. Y., 139 954–963 (2018). doi:10.1016/j.carbon.2018.08.009.
17) N.K. Maurya, V. Rastogi, and P. Singh, “Experimental and computational investigation on mechanical properties of reinforced additive manufactured component,” Evergreen, 6 (3) 207–214 (2019). doi:10.5109/2349296.
18) B. Dikici, and M. Gavgali, “The effect of sintering time on synthesis of in situ submicron α-al2o3 particles by the exothermic reactions of cuo particles in molten pure al,” J. Alloys Compd., 551 101–107 (2013). doi:10.1016/j.jallcom.2012.10.018.
19) S. Srivastava, and A. Srivastava, “Determination of halloysite reinforced/epoxy nanocomposite impact strength by experimental and computational procedures,” Evergreen, 11 (2) 729–735 (2024). doi:10.5109/7183352.
20) C.Liu, H. Zheng, X. Gu, B. Jiang, and J. Liang, “Effect of severe shot peening on corrosion behavior of az31 and az91 magnesium alloys,” J. Alloys Compd., 770 500–506 (2019). doi:10.1016/j.jallcom.2018.08.141.
21) M. Laleh, and F. Kargar, “Effect of surface nanocrystallization on the microstructural and corrosion characteristics of az91d magnesium alloy,” J. Alloys Compd., 509 (37) 9150–9156 (2011). doi:10.1016/j.jallcom.2011.06.094.
22) K. Xu, A. Wang, Y. Wang, X. Dong, X. Zhang, and Z. Huang, “Surface nanocrystallization mechanism of a rare earth magnesium alloy induced by hvof supersonic microparticles bombarding,” Appl. Surf. Sci., 256 (3) 619–626 (2009). doi:10.1016/j.apsusc.2009.06.098.
23) M. Laleh, A.S. Rouhaghdam, T. Shahrabi, and A. Shanghi, “Effect of alumina sol addition to micro-arc oxidation electrolyte on the properties of mao coatings formed on magnesium alloy az91d,” J. Alloys Compd., 496 (1–2) 548–552 (2010). doi:10.1016/j.jallcom.2010.02.098.
24) D. Luo, Y. Liu, X. Yin, H. Wang, Z. Han, and L. Ren, “Corrosion inhibition of hydrophobic coatings fabricated by micro-arc oxidation on an extruded mg–5sn–1zn alloy substrate,” J. Alloys Compd., 731 731–738 (2018). doi:10.1016/j.jallcom.2017.10.017.
25) B. Dikici, F. Bedir, and M. Gavgali, “The effect of high tic particle content on the tensile cracking and corrosion behavior of al–5cu matrix composites,” J.

Compos. Mater., 54 (13) 1681–1690 (2020). doi:10.1177/0021998319884098.

26) X. Gao, H. Yue, E. Guo, H. Zhang, X. Lin, L. Yao, and B. Wang, "Mechanical properties and thermal conductivity of graphene reinforced copper matrix composites," Powder Technol., 301 601–607 (2016). doi:10.1016/j.powtec.2016.06.045.
27) M. Cao, L. Liu, L. Fan, Z. Yu, Y. Li, E.E. Oguzie, and F. Wang, "Influence of temperature on corrosion behavior of 2a02 al alloy in marine atmospheric environments," Materials (Basel)., 11 (2) (2018). doi:10.3390/ma11020235.
28) O. Guler, and N. Bagci, "A short review on mechanical properties of graphene reinforced metal matrix composites," J. Mater. Res. Technol., 9 (3) 6808–6833 (2020). doi:10.1016/j.jmrt.2020.01.077.
29) D.G.Papageorgiou, I.A. Kinloch, and R.J. Young, "Mechanical properties of graphene and graphene-based nanocomposites," Prog. Mater. Sci., 90 75–127 (2017). doi:10.1016/j.pmatsci.2017.07.004.
30) S. Feng, Q. Guo, Z. Li, G. Fan, Z. Li, D.B. Xiong, Y. Su, Z. Tan, J. Zhang, and D. Zhang, "Strengthening and toughening mechanisms in graphene-al nanolaminated composite micro-pillars," Acta Mater., 125 98–108 (2017). doi:10.1016/j.actamat.2016.11.043.
31) J. Zhu, B. Jia, Y. Di, B. Liu, X. Wan, W. Wang, R. Tang, S. Liao, and X. Chen, "Effects of graphene content on the microstructure and mechanical properties of alumina-based composites," Front. Mater., 9 (2022). doi:10.3389/fmats.2022.965674.
32) M. Selvam, K. Saminathan, P. Siva, P. Saha, and V. Rajendran, "Corrosion behavior of mg/graphene composite in aqueous electrolyte," Mater. Chem. Phys., 172 129–136 (2016). doi:10.1016/j.matchemphys.2016.01.051.
33) Z. Li, J. Chu, C. Yang, S. Hao, M.A. Bissett, I.A. Kinloch, and R.J. Young, "Effect of functional groups on the agglomeration of graphene in nanocomposites," Compos. Sci. Technol., 163 116–122 (2018). doi:10.1016/j.compscitech.2018.05.016.
34) M. Rashad, F. Pan, A. Tang, M. Asif, J. She, J. Gou, J. Mao, and H. Hu, "Development of magnesium-graphene nanoplatelets composite," J. Compos. Mater., 49 (3) 285–293 (2015). doi:10.1177/0021998313518360.
35) X. Du, W. Du, Z. Wang, K. Liu, and S. Li, "Ultra-high strengthening efficiency of graphene nanoplatelets reinforced magnesium matrix composites," Mater. Sci. Eng. A, 711 633–642 (2018). doi:10.1016/j.msea.2017.11.040.
36) M. Rashad, F. Pan, and M. Asif, "Magnesium matrix composites reinforced with graphene nanoplatelets," Graphene Mater. Fundam. Emerg. Appl., 151–189 (2015). doi:10.1002/9781119131816.ch5.
37) S. Jayabharathy, and P. Mathiazhagan, "Investigation of mechanical and wear behaviour of az91 magnesium matrix hybrid composite with tio2/graphene," Mater. Today Proc., 27 2394–2397 (2019). doi:10.1016/j.matpr.2019.09.142.
38) S. Sharma, A. Handa, S.S. Singh, and D. Verma, "Influence of tool rotation speeds on mechanical and morphological properties of friction stir processed nano hybrid composite of mwcnt-graphene-az31 magnesium," J. Magnes. Alloy., 7 (3) 487–500 (2019). doi:10.1016/j.jma.2019.07.001.
39) V. Kavimani, K. Soorya Prakash, and T. Thankachan, "Multi-objective optimization in wedm process of graphene – sic-magnesium composite through hybrid techniques," Meas. J. Int. Meas. Confed., 145 335–349 (2019). doi:10.1016/j.measurement.2019.04.076.
40) L. Chen, Y. Zhao, H. Hou, T. Zhang, J. Liang, M. Li, and J. Li, "Development of az91d magnesium alloy-graphene nanoplatelets composites using thixomolding process," J. Alloys Compd., 778 359–374 (2019). doi:10.1016/j.jallcom.2018.11.148.
41) N.S. Subawa, N.W. Widhiasthini, I.P. Astawa, C. Dwiatmadja, and N.P.I. Permatasari, "The practices of virtual reality marketing in the tourism sector, a case study of bali, indonesia," Curr. Issues Tour., 24 (23) 3284–3295 (2021). doi:10.1080/13683500.2020.1870940.
42) I.P. Tussyadiah, D. Wang, T.H. Jung, and M.C. tom Dieck, "Virtual reality, presence, and attitude change: empirical evidence from tourism," Tour. Manag., 66 140–154 (2018). doi:10.1016/j.tourman.2017.12.003.

Cite: A. Tyagi, P. Kumar, "Microstructural and Mechanical Characterization of Magnesium-AZ31 Alloy Reinforced with Carbon Nanotubes and Nano-Hydroxyapatite". Evergreen, 12 (03) 1418-1425 (2025). https://doi.org/10.5109/7388838.